HHS Public Access

Author manuscript

J Invest Dermatol. Author manuscript; available in PMC 2018 November 08.

Published in final edited form as:

J Invest Dermatol. 2016 October ; 136(10): 2070–2079. doi:10.1016/j.jid.2016.06.013.

Overexpression of PRAS40^{T246A} in the Proliferative Compartment Suppresses mTORC1 Signaling, Keratinocyte Migration and Skin Tumor Development

Okkyung Rho[1], **Jaya Srivastava**[1], **Jiyoon Cho**[1], and **John DiGiovanni**[1,2]

[1]Division of Pharmacology and Toxicology, The University of Texas at Austin, 1400 Barbara Jordan Blvd. Austin, TX 78723

[2]Department of Nutritional Science, The University of Texas at Austin, 1400 Barbara Jordan Blvd. Austin, TX 78723

Abstract

The proline-rich Akt substrate of 40 kDa (PRAS40), an inhibitory component of the mTORC1 complex, was identified as an Akt substrate through phosphorylation at Thr246. Phosphorylation at this site releases PRAS40 from the mTORC1 complex allowing increased activity. Targeted expression of a mutant form of PRAS40 (PRAS40^{T246A}) in basal keratinocytes of mouse epidermis (BK5.PRAS40^{T246A} mice) has allowed further examination of mTORC1 specific signaling in epithelial carcinogenesis. BK5.PRAS40^{T246A} mice were resistant to TPA-induced epidermal hyperproliferation and skin tumor development. In transgenic mice, PRAS40^{T246A} remained bound to raptor in keratinocytes even after treatment with TPA, consistent with reduced mTORC1 signaling and altered levels of cell cycle proteins. BK5.PRAS40^{T246A} mice also displayed attenuated skin inflammation in response to TPA. Inhibition of mTORC1 in keratinocytes significantly inhibited their migration *in vitro* and, in addition, inhibited TPA-induced proliferation and migration of bulge-region stem cells *in vivo*. Furthermore, targeted inhibition of mTORC1 in BK5.PRAS40^{T246A} mice resulted in delayed wound healing. Decreased keratinocyte migration and impaired wound healing correlated with altered expression of EMT markers and reduced smad signaling. Collectively, the current data using this unique mouse model provide further evidence that mTORC1 signaling in keratinocytes regulates key events in keratinocyte function and epithelial cancer development.

Introduction

Considerable evidence exists for a role of Akt and mTOR signaling in cancer growth and progression (Forde and Dale, 2007, Guertin and Sabatini, 2005, Hay, 2005, Inoki et al. , 2005, Inoki and Guan, 2006, Mak and Yeung, 2004, Petroulakis et al. , 2006, Ruggero and Sonenberg, 2005). Previous studies from our laboratory revealed that Akt and mTORC1

To whom correspondence should be addressed: John DiGiovanni, Ph.D., Dell Pediatric Research Institute, The University of Texas at, Austin, 1400 Barbara Jordan Blvd. Austin, TX 78723. Phone: 512-495-4726. john.digiovanni@austin.utexas.edu.

Conflict of Interest

The authors declare no conflict of interest.

signaling pathways play an important role in epithelial carcinogenesis using the mouse skin model (Checkley et al. , 2011, Lu et al. , 2007). Rapamycin (an mTORC1 inhibitor) dramatically blocked mTORC1 downstream signaling, epidermal proliferation and skin tumor promotion induced by TPA in both wild-type (WT) and BK5.Akt1 transgenic mice (Checkley et al. , 2014, Checkley, Rho, 2011, Rho et al. , 2013). Treatment of mouse epidermis with TPA leads to increased phosphorylation of Akt and PRAS40 (proline-rich Akt substrate of 40 kDa) (Lu, Rho, 2007, Rho, Kiguchi, 2013).

PRAS40, an inhibitory subunit of mTORC1 was originally identified as an Akt substrate through Akt-mediated phosphorylation at Thr246 (Kovacina et al. , 2003, Vander Haar et al. , 2007) and this phosphorylation is critical for mTORC1 activity (Wang et al. , 2008, Wang et al. , 2007). Overexpression of PRAS40 and PRAS40 mutants (T246A or S221A) *in vitro* leads to inhibition of mTORC1 activity assessed by reduced phosphorylation of S6K1 at Thr389 and 4EBP1 at Thr37/46 (Oshiro et al. , 2007, Wang, Harris, 2008, Wang, Harris, 2007).

Here, we generated transgenic mice that overexpress a mutant form of PRAS40 ($PRAS40^{T246A}$) under control of the bovine keratin 5 (BK5) promoter to further examine the importance of keratinocyte specific mTORC1 signaling in epithelial carcinogenesis and to evaluate the functional contribution of mTORC1 during skin tumor promotion by TPA. Although BK5.$PRAS40^{T246A}$ mice did not display a discernable gross skin phenotype, these mice were significantly less sensitive to TPA-induced epidermal hyperproliferation and skin tumor development. In transgenic mice, $PRAS40^{T246A}$ remained bound to raptor in keratinocytes even after TPA treatment indicating a selective inhibition of mTORC1 signaling. BK5.$PRAS40^{T246A}$ mice exhibited reduced epidermal mTORC1 signaling and altered levels of cell cycle proteins consistent with reduced keratinocyte proliferation observed following treatment with TPA. BK5.$PRAS40^{T246A}$ mice also displayed a significantly reduced skin inflammatory response to TPA. Notably, TPA-mediated proliferation and migration of bulge-region label retaining cells (LRCs) were also inhibited in BK5.$PRAS40^{T246A}$ mice. Furthermore, expression of $PRAS40^{T246A}$ in basal keratinocytes significantly inhibited keratinocyte migration *in vitro* and led to delayed wound-healing. Finally, expression of $PRAS40^{T246A}$ modulated the levels of key EMT proteins in keratinocytes consistent with the effects observed on migration. Collectively, selective inhibition of mTORC1 signaling in keratinocytes of this unique mouse model has provided further evidence that mTORC1 signaling pathways regulate several important mechanistic events involved in the process of skin tumor development.

Results

Generation and initial characterization of BK5.$PRAS40^{T246A}$ mice

Using the BK5 vector, we generated transgenic mice that overexpress $PRAS40^{T246A}$ in basal keratinocytes of the epidermis to selectively inhibit keratinocyte mTORC1 signaling (Figure 1a). One line (L18) among five established lines had the highest epidermal expression of $PRAS40^{T246A}$ protein (Figure 1b, Figure S1a) and was bred to the FVB/J genetic background for all experiments. These mice did not have a histologically discernable skin

phenotype. Unless otherwise noted, all transgenic mice used for the study were hemizygous for the transgene.

Epidermal protein lysates were prepared from groups (n=5/group) of WT and BK5.PRAS40^{T246A} mice 6h after the last of 4 treatments with TPA (6.8 nmol) or acetone (Ace). Immunoprecipitation analysis showed that PRAS40 dissociation from raptor was induced by TPA treatment compared to Ace treatment in WT mice (ratio of TPA/Ace = 0.28) (Figures 1c, 1d). In contrast, overexpression of PRAS40^{T246A} in epidermis prevented dissociation of raptor following TPA treatment (ratio of TPA/Ace = 0.77).

Compared to WT mice, BK5.PRAS40^{T246A} mice displayed reduced epidermal mTORC1 downstream signaling as shown by reduced phosphorylation of S6K (Thr389), 4EBP1 (Ser65 and Thr37/46) and ULK1 (Ser757) (Figure 2a) at known mTORC1 phosphorylation sites (Fingar et al. , 2004, Rho et al. , 2011). No differences were observed in epidermal levels of phospho-PRAS40 (Thr246) and phospho-Akt (Ser473) following TPA treatment between PRAS40^{T246A} and WT mice as expected (Figure 2a). Quantitation of the levels of mTORC1 signaling in the Western blot shown in Figure 2a is provided in supplemental Figure S1b. We also compared the effects of various doses of rapamycin following topical treatment (200 nmol, 50 nmol, and 5 nmol) on TPA-induced mTORC1 signaling inhibition with that of BK5.PRAS40^{T246A} mice by measuring phosphorylation of S6K at Thr389. As shown in supplemental Figure S1b and S1c, reduction of TPA-induced mTORC1 activation in BK5.PRAS40^{T246A} mice produced a inhibitory effect similar to that observed with 5 nmol of rapamycin treatment. This dose of rapamycin was previously shown to produce an ~ 50% inhibition in skin tumor promotion by TPA in wild-type mice (Checkley *et al.*, 2011)

BK5.PRAS40^{T246A} mice also had reduced levels of phospho-Rb (Ser807/811) and reduced protein levels of Cdk2, Cdk6, Cyclin D3, Cyclin A and Cyclin E following treatment with TPA compared to WT mice (Figure 2b). In contrast, p27 protein levels were increased, while levels of Cdk4 and Cyclin D1 were not significantly altered compared to WT mice (Figures 2b, 2c). Figure 2c shows quantitative analysis of the levels of cell cycle proteins in BK5.PRAS40^{T246A} mice compared to WT mice 6h after TPA treatment. The reduced levels of Cdk6, Cdk2, Cyclin D3 and phospho-Rb following TPA treatment of BK5.PRAS40^{T246A} compared to WT mice were statistically significant (p=0.0011, Cdk6; p=0.0009, Cdk2; p=0.033, Cyclin D3; p=0.031, p-Rb, Student's t test).

We also analyzed additional key signaling pathways affecting the proliferative and survival responses in epidermis during TPA promotion. As shown in Figure S2, there were no significant differences in the signaling pathways examined suggesting a lack of significant off-target effects of transgene expression in these mice.

BK5.PRAS40^{T246A} mice are less sensitive to TPA-induced epidermal hyperproliferation, skin inflammation, and angiogenesis compared to WT mice

Groups of mice, 7 to 9 weeks of age, were topically treated with Ace or TPA (6.8 nmol) twice weekly for two weeks to compare the epidermal proliferative response. BrdU (100 μg/g) was injected 30 minutes prior to sacrifice. Skins were collected 48h after the last treatment for analysis of BrdU incorporation and inflammatory cell infiltrates in the dermis.

Representative BrdU stained skin sections are shown in Figure S3a. BK5.PRAS40^{T246A} mice were significantly less sensitive to TPA-induced epidermal hyperproliferation measured by labeling index (LI) and epidermal thickness (Figures 3a, 3b; $p<0.0001$, Mann-Whitney U test). These data together with the data in Figure 2 indicate that overexpression of PRAS40^{T246A} in basal keratinocytes effectively blocked TPA-induced epidermal hyperproliferation, which reproduces the effect of rapamycin observed in our previous studies (Checkley, Rho, 2011, Rho, Kiguchi, 2013).

There was a significant increase in the infiltration of mast cells (Toluidine Blue O staining, Figure S3b) and total leukocytes (CD45 staining, Figure S3c) in the dermis of WT mice following TPA treatment. However, these responses were significantly reduced in BK5.PRAS40^{T246A} mice (Figures 3c, 3d and Figures S3b, S3c). Quantitative RT-PCR (qRT-PCR) analysis revealed that mRNAs for IL-1α and TNFα were significantly reduced by 1.94-fold and 2.5-fold, respectively, in the epidermis of TPA-treated BK5.PRAS40^{T246A} mice compared to WT (Figure 3e; $p=0.016$ and $p=0.007$,respectively, Student's t test). In addition, the skin of BK5.PRAS40^{T246A} mice exhibited a markedly reduced angiogenic response after TPA treatment compared to WT mice (Figure S3d).

Targeting mTORC1 in keratinocytes effectively suppresses skin tumor promotion by TPA

Groups of 11–16 male and female mice 10–12 weeks of age were initiated with 50 nmol of DMBA. Two weeks after initiation, mice were treated topically (twice-weekly) with 6.8 nmol TPA or Ace. BK5.PRAS40^{T246A} mice displayed a significantly reduced tumor response. There was 63% inhibition at 22 weeks in the average number of papillomas per mouse in BK5.PRAS40^{T246A} mice compared to WT mice (Figure 4a; $p=0.0151$, Mann-Whitney U test). The final percent of mice with papillomas (tumor incidence) for WT and BK5.PRAS40^{T246A} was also significantly different at 22 weeks of promotion (Figure 4b; $p<0.0001$, χ^2 -test) and in addition, tumor latency was increased in BK5.PRAS40^{T246A} mice compared to the WT group (Figure S4a; $p=0.0008$, Mantel-Cox test). Finally, as shown in Figures 4c, 4d, **and** S4b, BK5.PRAS40^{T246A} mice exhibited reduced tumor size ($p=0.0041$, Mann-Whitney U test) as well as a significant decrease in tumor burden (i.e., tumor weight and total tumor weight per mouse) in BK5.PRAS40^{T246A} mice compared to WT mice ($p=0.0041$ and $p<0.0001$, respectively, Mann-Whitney U test).

Response of BK5.PRAS40^{T246A} mice to DMBA-Induced Epidermal Apoptosis

To determine whether expression of PRAS40^{T246A} influenced the epidermal response to DMBA, epidermal apoptosis was measured 24 h following a single topical dose of the tumor initiator (Figure S5). Apoptotic keratinocytes were analyzed in skin sections obtained by quantitating the number of active caspase-3 positive cells in both the interfollicular as well as follicular epidermis. As shown in Figure S5, there were no significant differences in the number of apoptotic keratinocytes in either epidermal compartment when comparing BK5.PRAS40^{T246A} mice to WT. These data suggest that the initiating response to DMBA (metabolism and DNA adduct formation) was not significantly affected in BK5.PRAS40^{T246A} mice.

Overexpression of PRAS40^{T246A} in basal keratinocytes blocks TPA-induced proliferation and migration of LRCs

To study the impact of selective mTORC1 inhibition in basal keratinocytes, BrdU (50 μg/gm) was injected *i.p.* to groups of 10 day-old pups every 12h for 2 days. At 11 weeks of age, the skins of BrdU injected mice were treated topically (twice-weekly for 2 weeks) with 6.8 nmol TPA or Ace and evaluated for BrdU staining and LRC analysis 48h following the last treatment as previously described (Rho, Kiguchi, 2013). The proliferation/migration of LRCs out of the hair follicle bulge region of TPA-treated BK5.PRAS40^{T246A} mice was significantly reduced (Figures S6, 5a; p=0.0143, Mann-Whitney U test) compared to WT mice. Most LRCs remained in or near the bulge region of BK5.PRAS40^{T246A} mice, while LRCs of WT mice had mostly migrated out of the bulge region.

Keratinocyte-specific expression of PRAS40^{T246A} inhibits keratinocyte migration and delays wound-healing.

Primary mouse keratinocytes were isolated, seeded evenly, and grown to confluence in collagen-coated 6-well culture plates. Cells were wounded by scratching and then incubated in complete medium for 24h to allow gap closure. An additional set of WT cells were treated with rapamycin (200 nM). As shown in Figure 5b and 5c, WT keratinocytes migrated into the scratched area within 24h whereas those from BK5.PRAS40^{T246A} mice and WT +Rapamycin did not. Furthermore, as shown in Figure 5d and Figure S7, BK5.PRAS40^{T246A} mice exhibited a significantly delayed wound-healing response following tape stripping at day 7 compared to WT mice (p=0.0318 Mann-Whitney U test). Therefore, selective mTORC1 inhibition in keratinocytes via expression of PRAS40^{T246A} blocked cell migration *in vitro* and wound healing *in vivo*. The effects on keratinocyte migration *in vitro* were mimicked by treatment with rapamycin.

We also investigated the expression of the key EMT markers, as EMT has been linked to tissue repair and remodeling (Corallino et al. , 2015). Mice were treated topically twice weekly for two weeks and epidermal tissue was harvested 6h following the last treatment. In the absence of TPA treatment, levels of the proteins shown were similar in epidermal lysates from WT and BK5.PRAS40^{T246A} mice (Figure 5e). In contrast, following treatment with TPA, increased levels of epithelial markers (E-cadherin, claudin-1, Fzd-7, Zo-1) and reduced levels of the mesenchymal marker, N- cadherin (Zeisberg and Neilson, 2009) were observed in BK5.PRAS40^{T246A} mice as compared with WT mice. The levels of twist1 and Tcf8/zeb1, which bind and suppress E-cadherin expression (Zeisberg and Neilson, 2009), were also reduced in TPA-treated epidermis of BK5.PRAS40^{T246A} (Figure 5e). Notably, the levels of MMP-9, Tspan13, and Wnt5a were markedly reduced in BK5.PRAS40^{T246A} in response to TPA compared to WT mice (Figure 5e).

Interestingly, the expression of nodal, a member of the TGFβ family was higher (both mRNA and protein) in TPA-treated epidermis of WT mice compared to BK5.PRAS40^{T246A} mice (Figures 5f, 5g). Smad signaling as assessed by phosphorylation of smad2 and smad3 was inhibited (especially phospho-smad3) in epidermis of BK5.PRAS40^{T246A} mice following treatment with TPA.

Discussion

A genetic approach, with targeted expression of PRAS40^{T246A} in basal keratinocytes (BK5.PRAS40^{T246A} mice), allowed for dissection of the role of mTORC1 specific signaling in keratinocytes during epithelial carcinogenesis. Our earlier studies demonstrated that topical treatment with rapamycin effectively reduced skin tumor promotion in both WT and BK5.Akt1^{WT} mice and inhibited further growth of existing papillomas as well as significantly inhibited skin inflammation (Checkley, Rho, 2011, Rho, Kiguchi, 2013). However, it could not be determined conclusively whether the effects of rapamycin on skin tumor promotion were due primarily to direct effects on keratinocytes or a combination of direct effects on keratinocytes and other cells that reside in the epidermis and dermis (e.g., inflammatory cells). Overexpression of PRSA40^{T246A} in basal keratinocytes caused a significant inhibition of epidermal proliferation and skin tumor promotion by TPA. The effect on tumor development was seen not only in tumor number, incidence, and tumor latency but also in tumor weight and size. These data using BK5.PRAS40^{T246A} mice mimic the effect of topical rapamycin on TPA-induced tumor promotion seen in our previous work (Checkley, Rho, 2011, Rho, Kiguchi, 2013). Our current and previous studies clearly demonstrate that inhibition of mTORC1 in keratinocytes is sufficient to inhibit both keratinocyte proliferation and skin tumor development induced by TPA.

Overexpression of PRAS40^{T246A} substantially prevented TPA-mediated dissociation of PRAS40 from raptor in the mTORC1 complex (Figures 1c, 1d) leading to inhibit epidermal mTORC1 signaling (Figure 2a). The levels of critical cell cycle proteins were altered in epidermis of BK5.PRAS40^{T246A} mice compared to WT mice treated with TPA (Figures 2b, 2c). Interestingly, the levels of Cdk4 and Cyclin D1 were not significantly changed in BK5.PRAS40^{T246A} mice compared to WT mice 6h after TPA treatment. Several previous studies have suggested that the Cdk6-Cyclin D3 complex can also initiate the G1/S transition (Connell-Crowley et al. , 1997, Faast et al. , 2004, Lin et al. , 2001). Thus, the changes observed in cell cycle regulatory proteins in PRAS40^{T246A} mice are consistent with the reduced proliferative response seen following TPA treatment and reduced tumor development. Recently, rapamycin given orally in a microencapsulated form (eRapa) was shown to inhibit two-stage skin carcinogenesis by inhibiting initiation with DMBA through a mechanism not involving inhibition of epidermal mTORC1 signaling (Dao et al. , 2015). In addition, eRapa did not inhibit tumor promotion by TPA in these studies. Thus, low dose rapamycin when given orally may have other effects that can influence the initiation of skin tumors independent of mTORC1 inhibition. However, in the current study we did not find evidence that expression of PRAS40^{T246A} in keratinocytes affected the apoptotic response to topical application of DMBA, which indirectly supports the hypothesis that inhibition of keratinocyte mTORC1 primarily impacted processes associated with tumor promotion in this model system.

To probe for possible off-target effects of overexpression of PRAS40^{T246A}, we analyzed several other signaling pathways in keratinocytes from both WT and BK5.PRAS40^{T246A} mice known to be important in skin tumor promotion by TPA (Rho, Kim, 2011). We did not find significant alterations in any of the signaling pathways examined, including Stat3, Erk, RSK, JNK, p-38 MAPK and Gsk3β. These data support the conclusion that

BK5.PRAS40^{T246A} mice represent a unique model of selective inhibition of mTORC1 signaling in basal keratinocytes of mouse epidermis.

In previous studies, topical rapamycin was shown to significantly inhibit the proliferation and upward migration of LRCs to the interfollicular epidermis following treatment with TPA (Rho, Kiguchi, 2013). As shown in Figure 5a **and** Figure S6, overexpression of PRAS40^{T246A} in basal keratinocytes (including those in the bulge region of hair follicles), significantly inhibited the proliferation and upward migration of LRCs from the hair follicle bulge region induced by TPA. Deng and colleagues demonstrated that mTORC1 signaling is essential for stem cell activation in hair follicles (Deng et al. , 2015). In addition, Castilho *et al* (Castilho et al. , 2009) reported that rapamycin treatment retained CD34^{+} keratinocyte stem cells (KSCs) in the bulge region of the hair follicle of K5rtTA/tet-Wnt1 transgenic mice. Furthermore, Rodgers *et al* (Rodgers et al. , 2014) demonstrated that mTORC1 activity was essential for the transition of quiescent adult stem cells into an “alert” phase to enter the cell cycle in response to injury and stress. Our data support the hypothesis that mTORC1 contributes significantly to the proliferation and migration of bulge-region KSCs.

Interestingly, mTORC1 signaling has been implicated in the migration of several epithelial cell types (Kim et al. , 2012, Liu et al. , 2012). In K14.Cre x PTEN$^{flox/flox}$ mice, wound-healing and keratinocyte migration are increased, which are inhibited by rapamycin (Squarize et al. , 2010). Activation of mTORC1 in keratinocytes of K14.Cre x Tsc1$^{flox/flox}$ mice has been shown to accelerate cutaneous wound-healing as compared to control mice (Squarize, Castilho, 2010). In our study, mTORC1 inhibition by overexpression of PRAS40^{T246A} dramatically inhibited migration of keratinocytes *in vitro* and delayed wound-healing *in vivo* (see again Figures 5b, 5c, 5d and Figure S7). Rapamycin also effectively inhibited keratinocyte migration in vitro. Moreover, we examined the levels of key EMT markers linked to tissue remodeling and repair (Corallino, Malabarba, 2015, Xu et al. , 2009). Increased levels of the epithelial markers as well as decreased levels of a mesenchymal marker were found in epidermis of BK5.PRAS40^{T246A} mice compared to WT mice following treatment with TPA (Figure 5e). Cells with reduced Fzd7, a seven-pass trans-membrane Wnt receptor could not undergo mesenchymal-epithelial transition causing a mesenchymal state in colorectal cancer cells (Vincan et al. , 2007). As seen in Figure 5e, Fzd7 protein was elevated in epidermis of BK5.PRAS40^{T246A} compared to WT after TPA treatment. Wnt5a signaling is linked to cell motility and invasion in various tumors (Kurayoshi et al. , 2006, Ripka et al. , 2007, Weeraratna et al. , 2002). TPA induced Wnt5a expression in epidermis of WT but not BK5.PRAS40^{T246A} mice (Figure 5e). MMP-9 is associated with keratinocyte migration and wound-repair in mouse skin (Hattori et al. , 2009, LeBert et al. , 2015, McCawley et al. , 1998). Reduced MMP-9 expression leads to impaired wound-healing and reduced migration of keratinocytes. Induction of MMP-9 expression in mouse epidermis by TPA was significantly inhibited in BK5.PRAS40^{T246A} mice as compared with WT (Figure 5e). Tspan13, a member of the tetraspanin superfamily is associated in cell adhesion and migration (Serru et al. , 2000). Tspan13 protein levels were also significantly reduced in epidermis of BK5.PRAS40^{T246A} mice compared with WT mice following TPA treatment (Figure 5e). Collectively, the current data demonstrate that the

PRAS40^{T246A} expression in basal keratinocytes resulted in decreased migration, increased adhesion and impaired wound-healing.

TPA-induced expression of nodal, a member of the TGFβ family (Zhou et al. , 1993) was significantly inhibited in epidermis of BK5.PRAS40^{T246A} compared to WT (Figures 5f, 5g). Nodal is involved in embryonic development and is important for maintaining self-renewal and pluripotency in human embryonic stem cells (Vallier et al. , 2005, Vallier et al. , 2004). These functions occur through binding to specific cell surface receptors and activation of signaling via smad2/3 (Shi and Massague, 2003). Recent studies have described that nodal induces EMT and invasion in murine melanoma cells both *in vitro* and *in vivo* (Guo et al. , 2015, Quail et al. , 2014). As demonstrated in Figure 5f, phosphorylation of smad3 was significantly reduced in epidermis of BK5.PRAS40^{T246A} mice after TPA treatment compared to WT mice. These data are consistent with the reduced levels of nodal and thus changes in this signaling pathway may also play a role in the reduced migratory properties of keratinocytes in BK5.PRAS40^{T246A} mice.

Finally, in our previous study, topical application of rapamycin to the skin inhibited the TPA-induced infiltration of inflammatory cells including T cells, macrophages, neutrophils and mast cells (Checkley, Rho, 2011). In the present study, inhibition of mTORC1 signaling in basal keratinocytes of BK5.PRAS40^{T246A} mice significantly reduced dermal infiltration of inflammatory cells including mast cells and total leukocytes following TPA treatment (Figures 3c, 3d, S3b, S3c). Furthermore, the expression of inflammatory cytokines induced in the epidermis of WT mice by TPA treatment, specifically IL-1α and TNFα, was downregulated in BK5.PRAS40^{T246A} mice (Figure 3e). In addition, TPA-induced neovascularization as visualized by CD31 staining was dramatically inhibited in the skin of BK5.PRAS40^{T246A} mice compared to WT mice (Figure S3d). Thus, mTORC1 signaling in keratinocytes plays a crucial role in regulating the dermal inflammatory/angiogenesis response to TPA, in part, by regulating the levels of cytokines that they produced.

In conclusion, the current data clearly demonstrate that selective blocking of mTORC1 in keratinocytes is sufficient to produce inhibition of skin tumor promotion, wound-healing and skin inflammation. These studies further show that mTORC1 is an important target for cancer prevention and that BK5.PRAS40^{T246A} mice represent a unique model for further studies on mTORC1 specific signaling in cancer development.

Materials and Methods

Chemicals and Reagents.

DMBA, BrdU, anti-β-tubulin, anti-actin, proteinase inhibitor cocktails, and phosphatase inhibitor cocktails were purchased from Sigma. TPA and Zinc Fixative were obtained from Alexis Corporation or BD Transduction Laboratories, respectively. Antibodies were purchased from Cell Signaling Technology except Cyclin A (Santa Cruz Biotechnology), p27 (BD Transduction Laboratories) and CD31 (Abcam).

Generation of BK5.PRAS40^{T246A} mice.

Transgenic mice that overexpress PRAS40^{T246A} were generated using the BK5 vector as previously described(Bol et al. , 1998, Segrelles et al. , 2007). The PRAS40^{T246A} plasmid was generously provided by Lifu Wang (University of Virginia, Charlottesville, VA)(Wang, Harris, 2008). Transgenic mice were generated on a FVB/N genetic background in the Mouse Genetic Engineering Facility at The University of Texas at Austin and then transferred to a FVB/J mice (The Jackson Laboratory, Bar Harbor, ME) for all experiments.

Animals and Treatments.

Mice were fed *ad libitum* and group housed for all experiments. Preparation of epidermal protein lysates and analysis of epidermal thickness and LI were conducted as previously described(Rho, Kiguchi, 2013).

Immunohistochemistry and Toluidine Blue O staining.

The expression of PRAS40, CD45, and CD31 were analyzed using immunofluorescence on skin sections as described(Kim et al. , 2009). For CD45 and CD31 staining, sections fixed in zinc fixative were generated from paraffin-embedded skins. For Toluidine Blue O staining, paraffin-embedded sections were deparaffinized and stained in 1% Toluidine Blue O for 1 minute. After washing and dehydration, slides mounted with VectaMount mounting media(Checkley, Rho, 2011).

qRT-PCR Detection of Cytokines..

cDNAs from RNA isolated using the Qiagen RNeasy Mini Kit were synthesized by Superscript III reverse transcriptase (Invitrogen). qRT-PCR was carried out with Assay-On-Demand TaqMan probes [TNF α (Mm0043258), IL-1 α (Mm00439620), and Rn18s (Mm03928990)] (Applied Biosystems) using ViiA ™ 7 Real-Time PCR System.

Two-Stage Skin Carcinogenesis.

Groups of 11–16 male and female mice were initiated with 50 nmol of DMBA. Two weeks after initiation, mice received twice-weekly topical treatments with TPA (6.8 nmol) or Ace. Tumor multiplicity (average number of papillomas per mouse) and tumor incidence were recorded weekly until tumor multiplicity reached a plateau.

Wound-Healing Assays.

Primary mouse keratinocytes were isolated as previously described(Macias et al. , 2014), seeded evenly, and grown to confluence in collagen-coated 6-well culture plates. Cells were wounded by scratching with a 200 μl tip and incubated in complete medium for 24h. For tape stripping-wound of skin, 3M Scotch tape was applied and lifted from the shaved back skin 30 times to remove the epidermal stratum corneum. Area with lesion was measured for 7day period.

LRC Analysis:

BrdU (50 μg/g body weight) was injected to 10 day-old pups and treated as described(Rho, Kiguchi, 2013). Dorsal skins were collected 48h after the last treatment, processed and stained for BrdU.

Statistical Analysis.

For comparisons of epidermal thickness, LI, tumor multiplicity, tumor size, wound-healing assay, and LRCs, the one-tailed Mann-Whitney *U*-test was used. For qRT-PCR and the levels of cell cycle proteins, significance of changes was determined by a two-tailed Student's *t* test. To compare tumor incidence, the χ^2 test was used. For tumor latency comparison, the one-tailed log-rank (Mantel-Cox) test was used. GraphPad Prism was used for all statistical tests, and significance was set at $p \leq 0.05$.

Supplementary Material

Refer to Web version on PubMed Central for supplementary material.

Acknowledgements

This work was supported by NIH Grants CA164159 and American Cancer Research Center and Foundation. J. Srivastava was supported by the Cancer Prevention and Research Institute of Texas Training Grant RP140108.

References

Bol D, Kiguchi K, Beltran L, Rupp T, Moats S, Gimenez-Conti I, et al. Severe follicular hyperplasia and spontaneous papilloma formation in transgenic mice expressing the neu oncogene under the control of the bovine keratin 5 promoter. Mol Carcinog 1998;21:2–12. [PubMed: 9473766]

Castilho RM, Squarize CH, Chodosh LA, Williams BO, Gutkind JS. mTOR mediates Wnt-induced epidermal stem cell exhaustion and aging. Cell Stem Cell 2009;5:279–89. [PubMed: 19733540]

Checkley LA, Rho O, Angel JM, Cho J, Blando J, Beltran L, et al. Metformin inhibits skin tumor promotion in overweight and obese mice. Cancer Prev Res (Phila) 2014;7:54–64. [PubMed: 24196830]

Checkley LA, Rho O, Moore T, Hursting S, DiGiovanni J. Rapamycin is a potent inhibitor of skin tumor promotion by 12-O-tetradecanoylphorbol-13-acetate. Cancer Prev Res (Phila) 2011;4:1011–20. [PubMed: 21733825]

Connell-Crowley L, Harper JW, Goodrich DW. Cyclin D1/Cdk4 regulates retinoblastoma protein-mediated cell cycle arrest by site-specific phosphorylation. Mol Biol Cell 1997;8:287–301. [PubMed: 9190208]

Corallino S, Malabarba MG, Zobel M, Di Fiore PP, Scita G. Epithelial-to-Mesenchymal Plasticity Harnesses Endocytic Circuitries. Front Oncol 2015;5:45. [PubMed: 25767773]

Dao V, Pandeswara S, Liu Y, Hurez V, Dodds S, Callaway D, et al. Prevention of carcinogen and inflammation-induced dermal cancer by oral rapamycin includes reducing genetic damage. Cancer Prev Res (Phila) 2015;8:400–9. [PubMed: 25736275]

Deng Z, Lei X, Zhang X, Zhang H, Liu S, Chen Q, et al. mTOR signaling promotes stem cell activation via counterbalancing BMP-mediated suppression during hair regeneration. J Mol Cell Biol 2015;7:62–72. [PubMed: 25609845]

Faast R, White J, Cartwright P, Crocker L, Sarcevic B, Dalton S. Cdk6-cyclin D3 activity in murine ES cells is resistant to inhibition by p16(INK4a). Oncogene 2004;23:491–502. [PubMed: 14724578]

Fingar DC, Richardson CJ, Tee AR, Cheatham L, Tsou C, Blenis J. mTOR controls cell cycle progression through its cell growth effectors S6K1 and 4E-BP1/eukaryotic translation initiation factor 4E. Mol Cell Biol 2004;24:200–16. [PubMed: 14673156]

Forde JE, Dale TC. Glycogen synthase kinase 3: a key regulator of cellular fate. Cell Mol Life Sci 2007;64:1930–44. [PubMed: 17530463]

Guertin DA, Sabatini DM. An expanding role for mTOR in cancer. Trends Mol Med 2005;11:353–61. [PubMed: 16002336]

Guo Q, Ning F, Fang R, Wang HS, Zhang G, Quan MY, et al. Endogenous Nodal promotes melanoma undergoing epithelial-mesenchymal transition via Snail and Slug in vitro and in vivo. Am J Cancer Res 2015;5:2098–112. [PubMed: 26269769]

Hattori N, Mochizuki S, Kishi K, Nakajima T, Takaishi H, D'Armiento J, et al. MMP-13 plays a role in keratinocyte migration, angiogenesis, and contraction in mouse skin wound healing. Am J Pathol 2009;175:533–46. [PubMed: 19590036]

Hay N The Akt-mTOR tango and its relevance to cancer. Cancer Cell 2005;8:179–83. [PubMed: 16169463]

Inoki K, Corradetti MN, Guan KL. Dysregulation of the TSC-mTOR pathway in human disease. Nat Genet 2005;37:19–24. [PubMed: 15624019]

Inoki K, Guan KL. Complexity of the TOR signaling network. Trends Cell Biol 2006;16:206–12. [PubMed: 16516475]

Kim DJ, Angel JM, Sano S, DiGiovanni J. Constitutive activation and targeted disruption of signal transducer and activator of transcription 3 (Stat3) in mouse epidermis reveal its critical role in UVB-induced skin carcinogenesis. Oncogene 2009;28:950–60. [PubMed: 19137019]

Kim YW, Lee WH, Choi SM, Seo YY, Ahn BO, Kim SH, et al. DA6034 promotes gastric epithelial cell migration and wound-healing through the mTOR pathway. J Gastroenterol Hepatol 2012;27:397–405. [PubMed: 21793913]

Kovacina KS, Park GY, Bae SS, Guzzetta AW, Schaefer E, Birnbaum MJ, et al. Identification of a proline-rich Akt substrate as a 14–3-3 binding partner. J Biol Chem 2003;278:10189–94. [PubMed: 12524439]

Kurayoshi M, Oue N, Yamamoto H, Kishida M, Inoue A, Asahara T, et al. Expression of Wnt-5a is correlated with aggressiveness of gastric cancer by stimulating cell migration and invasion. Cancer Res 2006;66:10439–48. [PubMed: 17079465]

LeBert DC, Squirrell JM, Rindy J, Broadbridge E, Lui Y, Zakrzewska A, et al. Matrix metalloproteinase 9 modulates collagen matrices and wound repair. Development 2015;142:2136–46. [PubMed: 26015541]

Lin J, Jinno S, Okayama H. Cdk6-cyclin D3 complex evades inhibition by inhibitor proteins and uniquely controls cell's proliferation competence. Oncogene 2001;20:2000–9. [PubMed: 11360184]

Liu Y, Cao GF, Xue J, Wan J, Wan Y, Jiang Q, et al. Tumor necrosis factor-alpha (TNF-alpha)-mediated in vitro human retinal pigment epithelial (RPE) cell migration mainly requires Akt/mTOR complex 1 (mTORC1), but not mTOR complex 2 (mTORC2) signaling. Eur J Cell Biol 2012;91:728–37. [PubMed: 22595285]

Lu J, Rho O, Wilker E, Beltran L, DiGiovanni J. Activation of Epidermal Akt by Diverse Mouse Skin Tumor Promotion. Molecular Cancer Res 2007:1342–52.

Macias E, Rao D, Carbajal S, Kiguchi K, DiGiovanni J. Stat3 binds to mtDNA and regulates mitochondrial gene expression in keratinocytes. J Invest Dermatol 2014;134:1971–80. [PubMed: 24496235]

Mak BC, Yeung RS. The tuberous sclerosis complex genes in tumor development. Cancer Invest 2004;22:588–603. [PubMed: 15565817]

McCawley LJ, O'Brien P, Hudson LG. Epidermal growth factor (EGF)- and scatter factor/hepatocyte growth factor (SF/HGF)- mediated keratinocyte migration is coincident with induction of matrix metalloproteinase (MMP)-9. J Cell Physiol 1998;176:255–65. [PubMed: 9648913]

Oshiro N, Takahashi R, Yoshino K, Tanimura K, Nakashima A, Eguchi S, et al. The proline-rich Akt substrate of 40 kDa (PRAS40) is a physiological substrate of mammalian target of rapamycin complex 1. J Biol Chem 2007;282:20329–39. [PubMed: 17517883]

Petroulakis E, Mamane Y, Le Bacquer O, Shahbazian D, Sonenberg N. mTOR signaling: implications for cancer and anticancer therapy. Br J Cancer 2006;94:195–9. [PubMed: 16404421]

Quail DF, Zhang G, Findlay SD, Hess DA, Postovit LM. Nodal promotes invasive phenotypes via a mitogen-activated protein kinase-dependent pathway. Oncogene 2014;33:461–73. [PubMed: 23334323]

Rho O, Kiguchi K, Jiang G, Digiovanni J. Impact of mTORC1 inhibition on keratinocyte proliferation during skin tumor promotion in wild-type and BK5.Akt mice. Mol Carcinog 2013;53:871–82. [PubMed: 24114993]

Rho O, Kim DJ, Kiguchi K, Digiovanni J. Growth factor signaling pathways as targets for prevention of epithelial carcinogenesis. Mol Carcinog 2011;50:264–79. [PubMed: 20648549]

Ripka S, Konig A, Buchholz M, Wagner M, Sipos B, Kloppel G, et al. WNT5A--target of CUTL1 and potent modulator of tumor cell migration and invasion in pancreatic cancer. Carcinogenesis 2007;28:1178–87. [PubMed: 17227781]

Rodgers JT, King KY, Brett JO, Cromie MJ, Charville GW, Maguire KK, et al. mTORC1 controls the adaptive transition of quiescent stem cells from G0 to G(Alert). Nature 2014;510:393–6. [PubMed: 24870234]

Ruggero D, Sonenberg N. The Akt of translational control. Oncogene 2005;24:7426–34. [PubMed: 16288289]

Segrelles C, Lu J, Hammann B, Santos M, Moral M, Cascallana JL, et al. Deregulated activity of Akt in epithelial basal cells induces spontaneous tumors and heightened sensitivity to skin carcinogenesis. Cancer Res 2007;67:10879–88. [PubMed: 18006833]

Serru V, Dessen P, Boucheix C, Rubinstein E. Sequence and expression of seven new tetraspans. Biochim Biophys Acta 2000;1478:159–63. [PubMed: 10719184]

Shi Y, Massague J. Mechanisms of TGF-beta signaling from cell membrane to the nucleus. Cell 2003;113:685–700. [PubMed: 12809600]

Squarize CH, Castilho RM, Bugge TH, Gutkind JS. Accelerated wound healing by mTOR activation in genetically defined mouse models. PLoS One 2010;5:e10643. [PubMed: 20498714]

Vallier L, Alexander M, Pedersen RA. Activin/Nodal and FGF pathways cooperate to maintain pluripotency of human embryonic stem cells. J Cell Sci 2005;118:4495–509. [PubMed: 16179608]

Vallier L, Reynolds D, Pedersen RA. Nodal inhibits differentiation of human embryonic stem cells along the neuroectodermal default pathway. Dev Biol 2004;275:403–21. [PubMed: 15501227]

Vander Haar E, Lee SI, Bandhakavi S, Griffin TJ, Kim DH. Insulin signalling to mTOR mediated by the Akt/PKB substrate PRAS40. Nat Cell Biol 2007;9:316–23. [PubMed: 17277771]

Vincan E, Darcy PK, Farrelly CA, Faux MC, Brabletz T, Ramsay RG. Frizzled-7 dictates three-dimensional organization of colorectal cancer cell carcinoids. Oncogene 2007;26:2340–52. [PubMed: 17016432]

Wang L, Harris TE, Lawrence JC, Jr. Regulation of proline-rich Akt substrate of 40 kDa (PRAS40) function by mammalian target of rapamycin complex 1 (mTORC1)-mediated phosphorylation. J Biol Chem 2008;283:15619–27. [PubMed: 18372248]

Wang L, Harris TE, Roth RA, Lawrence JC, Jr. PRAS40 regulates mTORC1 kinase activity by functioning as a direct inhibitor of substrate binding. J Biol Chem 2007;282:20036–44. [PubMed: 17510057]

Weeraratna AT, Jiang Y, Hostetter G, Rosenblatt K, Duray P, Bittner M, et al. Wnt5a signaling directly affects cell motility and invasion of metastatic melanoma. Cancer Cell 2002;1:279–88. [PubMed: 12086864]

Xu J, Lamouille S, Derynck R. TGF-beta-induced epithelial to mesenchymal transition. Cell Res 2009;19:156–72. [PubMed: 19153598]

Zeisberg M, Neilson EG. Biomarkers for epithelial-mesenchymal transitions. J Clin Invest 2009;119:1429–37. [PubMed: 19487819]

Zhou X, Sasaki H, Lowe L, Hogan BL, Kuehn MR. Nodal is a novel TGF-beta-like gene expressed in the mouse node during gastrulation. Nature 1993;361:543–7. [PubMed: 8429908]

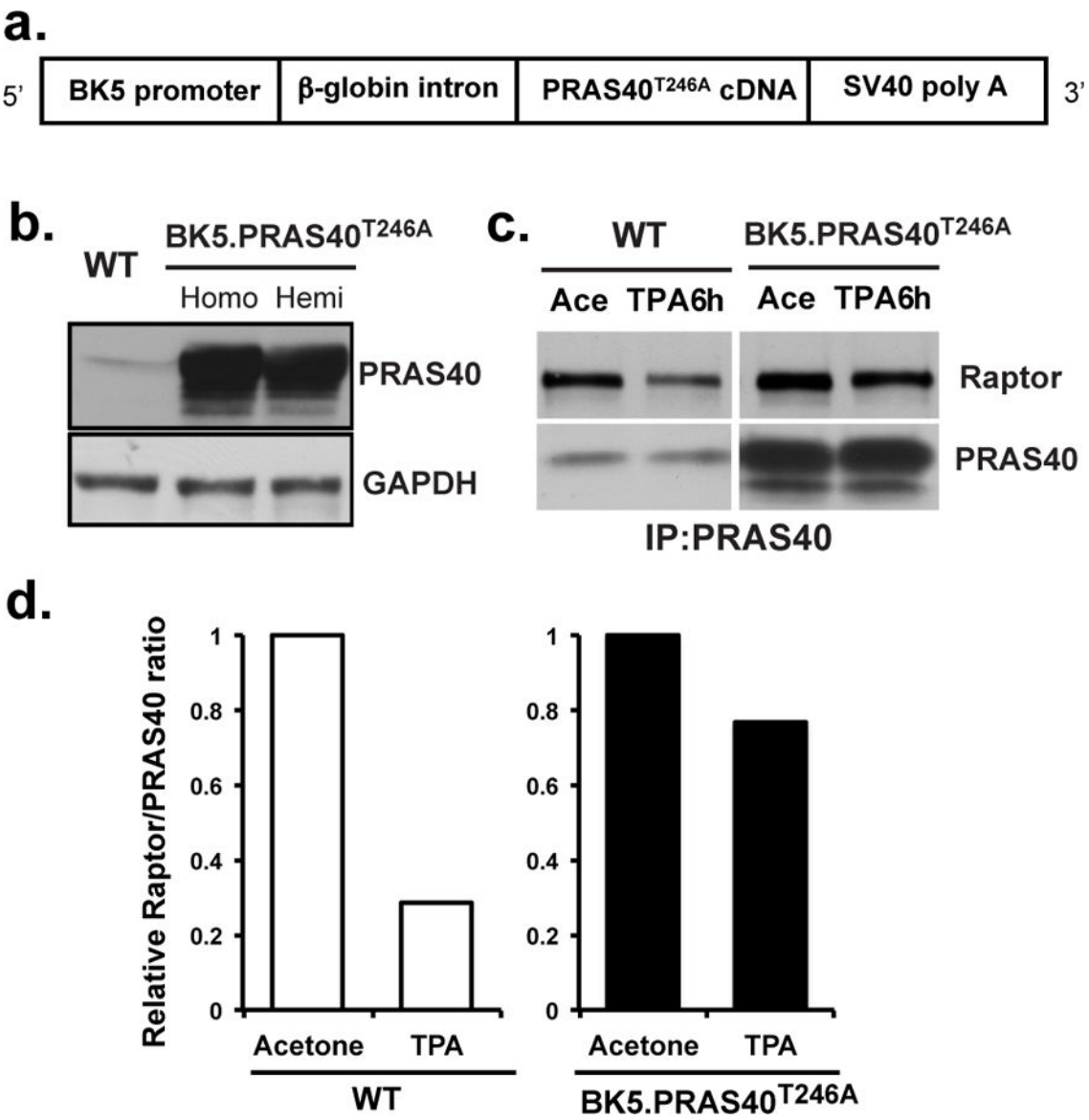

Figure 1. Generation and characterization of BK5.PRAS40^{T246A} transgenic mouse lines.

(a), Schematic of the construct used to generate the PRAS40 mutant (PRAS40^{T246A}) transgenic mice using the BK5 promoter. (b), Western analysis of PRAS40 protein levels in epidermis of WT and homozygous (Homo) and hemizygous (Hemi) BK5.PRAS40^{T246A} mice. (c), Effect of PRAS40^{T246A} on association with raptor. Epidermal protein lysates were prepared from WT and BK5.PRAS40^{T246A} mice (n=5/group) after multiple (4X) treatments with TPA (6.8 nmol). Mice were sacrificed 6 h after the final treatment of either TPA or Ace. PRAS40 proteins were immunoprecipitated and probed with raptor or PRAS40 antibody. Initial experiments using an IgG control did not reveal any specific bands in the regions where raptor or PRAS40 migrated in the gels. (d), Quantitative analysis of the effect of overexpression of PRAS40^{T246A} on the interactions of PRAS40 with raptor in the mTORC1 complex with and without TPA treatment.

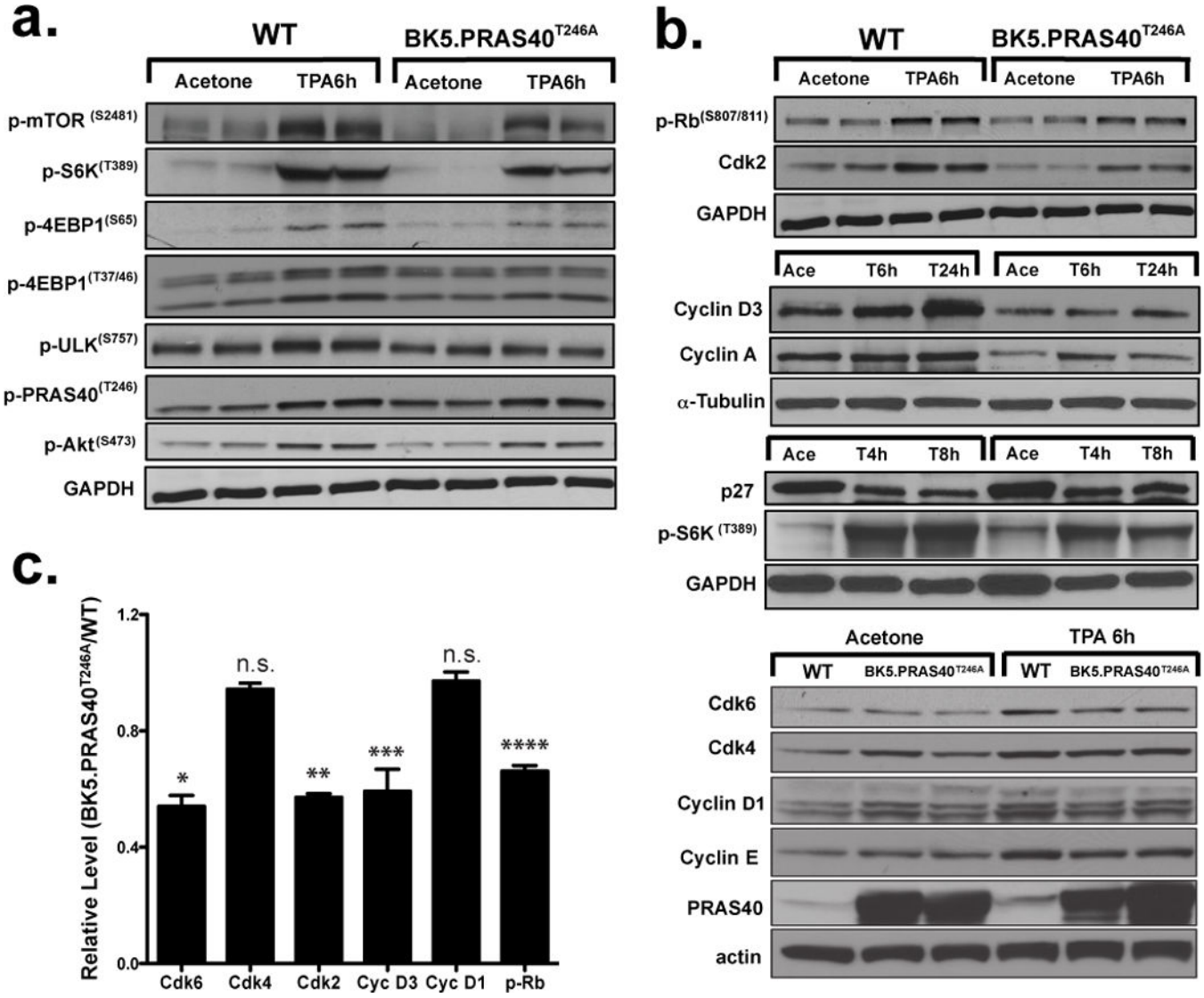

Figure 2. Impact of PRAS40^{T246A} overexpression in keratinocytes on mTORC1 signaling and cell cycle proteins following treatment with TPA.

(a), Western blot analysis of epidermal mTORC1 signaling in BK5.PRAS40^{T246A} mice following multiple (4X) treatments with TPA or acetone (Ace). Epidermal protein lysates were prepared from mice sacrificed 6 h after the final treatment. (b), Representative Western analysis of cell cycle regulatory proteins in epidermis of BK5.PRAS40^{T246A} and WT mice at the indicated time point following multiple treatments. (c), Quantitative analysis of the levels of cell cycle regulatory proteins in BK5.PRAS40^{T246A} mice compared to WT mice 6 h after TPA treatment. Values in the graph are expressed as mean ± SEM. n.s., not significant; *p=0.0011, Cdk6; **p=0.0009, Cdk2; ***p=0.033, Cyclin D3; ****p=0.031, p-Rb (Student's t test).

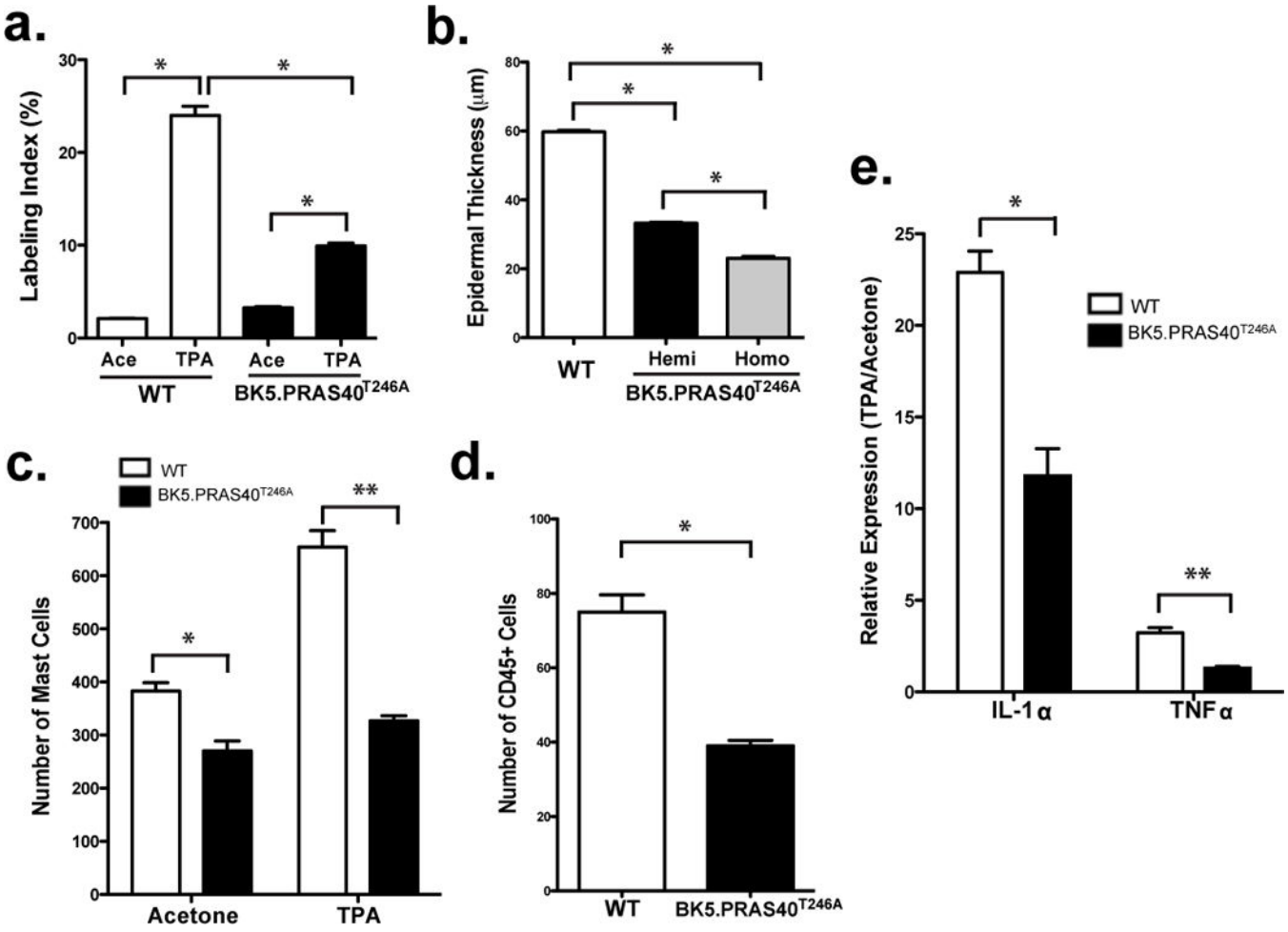

Figure 3. Suppressed epidermal hyperproliferation and dermal infiltration of inflammatory cells by TPA in BK5.PRAS40^{T246A} mice.

Mice were treated twice-weekly for 2 weeks with Ace or TPA (6.8 nmol). Skins injected with BrdU were collected 48h after the last treatment for analysis of BrdU incorporation and inflammatory cells. Values in the graphs are expressed as mean ± SEM (n≥3/group). (a), Quantitation of epidermal labeling index (LI). *p<0.0001 (b), Quantitation of epidermal thickness. *p<0.0001 (c), Mast cell staining with Toluidine Blue O. *p=0.0011, **p=0.0025 (d), Total leukocyte staining with CD45 antibody. *p=0.05 (e), qRT-PCR analysis of IL-1α and TNFα in epidermis of WT and BK5.PRAS40^{T246A}. RNA was normalized to 18s ribosomal RNA. Relative expression (TPA/Ace) values from 4 mice per group are shown. *p=0.016 and **p=0.007

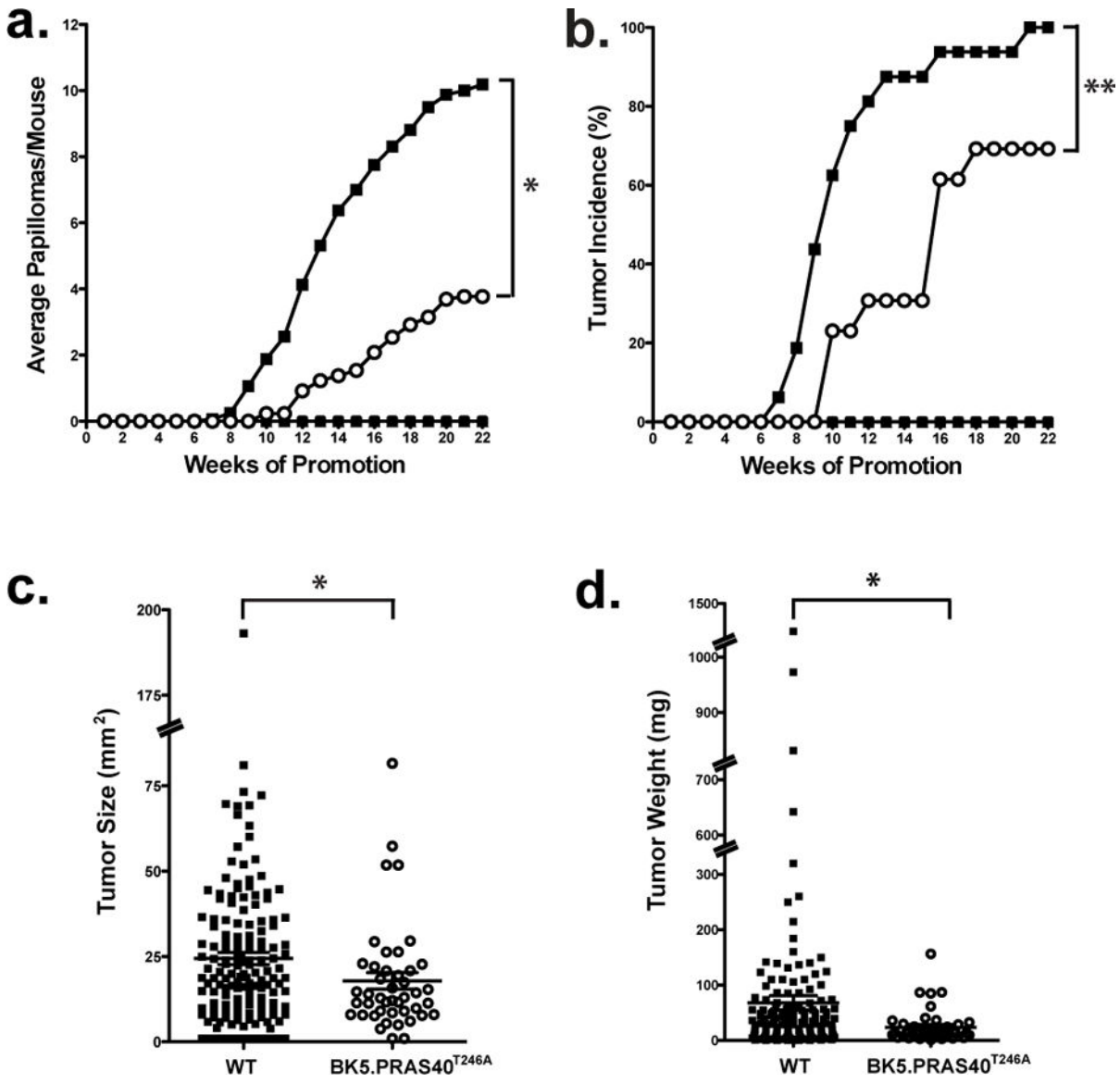

Figure 4. Effect of PRAS40^{T246A} overexpression in basal keratinocytes on skin tumor promotion.

Mice 10–12 weeks of age were initiated with 50 nmol of DMBA. Two weeks after initiation, mice were treated topically twice weekly with 6.8 nmol TPA or Ace for 22 weeks. (a), Tumor multiplicity. DMBA/Acetone (□) and DMBA/TPA (■) of WT mice; DMBA/Acetone (▲) and DMBA/TPA (O) of BK5.PRAS40^{T246A} mice. *p=0.0151 (b), Tumor incidence. **p<0.0001 (c), Evaluation of tumor size for both WT (DMBA/TPA, ■) and BK5.PRAS40^{T246A} (DMBA/TPA, O) mice. The size of each skin tumor (mm^2) was measured with an electronic caliper at 22 weeks. Graphs represent the average surface area ± SEM. *p=0.0041 (d), Measurement of tumor weight (mg) for WT (DMBA/TPA, ■) and BK5.PRAS40^{T246A} (DMBA/TPA, O) mice. *p=0.0041

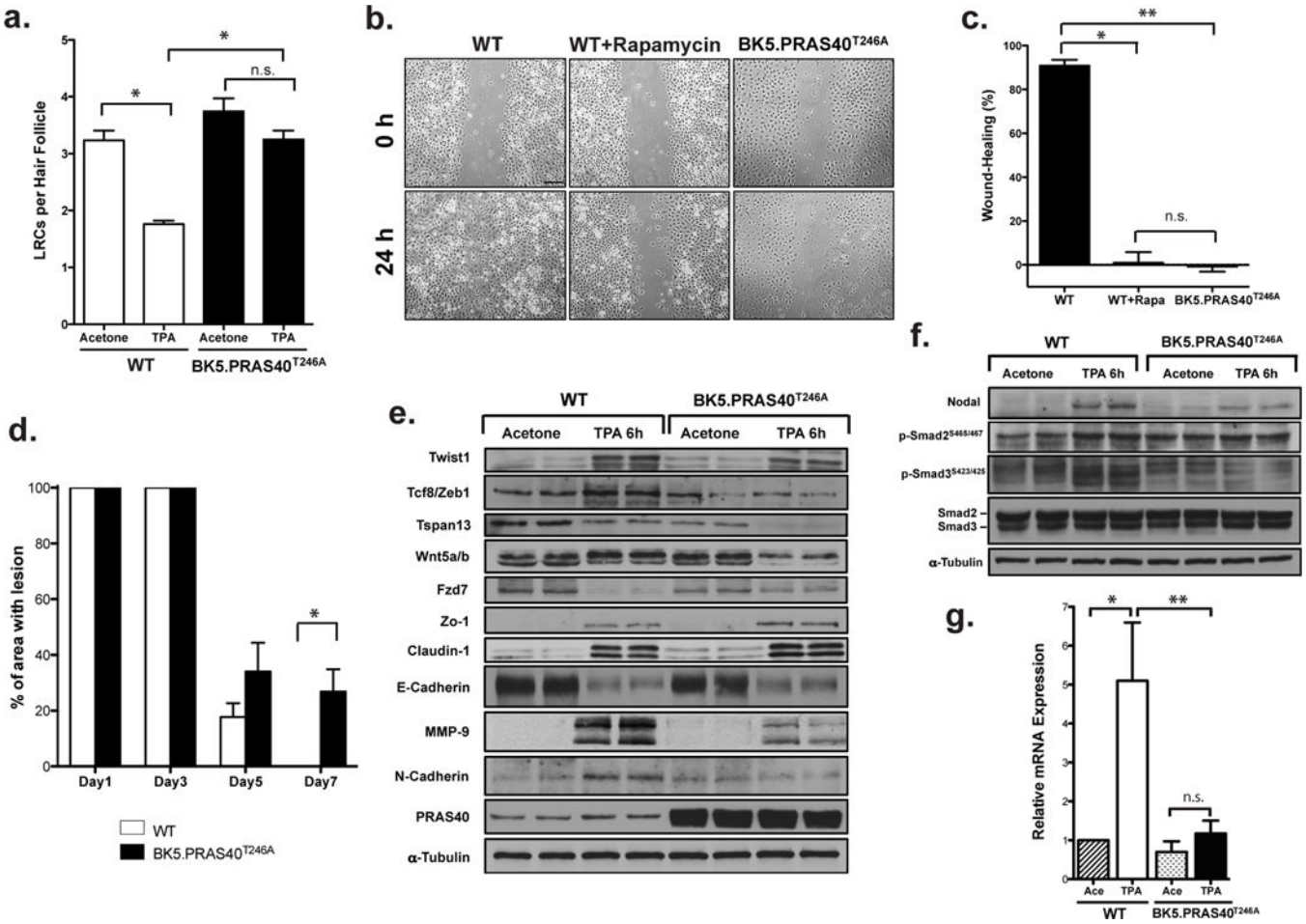

Figure 5. Effect of PRAS40^{T246A} in TPA-induced proliferation/migration of LRCs.

Values in the graph are expressed as mean ± SEM (n≥3/group). n.s.;not significant (a), Quantitation of LRCs per hair follicle. Skin sections stained with BrdU in the hair follicles (Figure S6). The BrdU positive cells per hair follicle were counted in at least 3 skin sections per mouse. *p=0.0143 (b), *In vitro* wound-healing assay. Scale bar, 20 μm. (c), Quantitation of the percentage of gap closure for *in vitro* wound-healing. *p=0.0004; **p=0.0002 (d), Quantitation of wound-healing response after tape-stripping measured by percentage of the area with lesion. *p=0.0318 (e, f). Western blot analysis of EMT proteins (e) and nodal signaling (f) in epidermis. (g) qRT-PCR of Nodal mRNA expression from 3 mice. *p=0.0084; **p=0.0083.